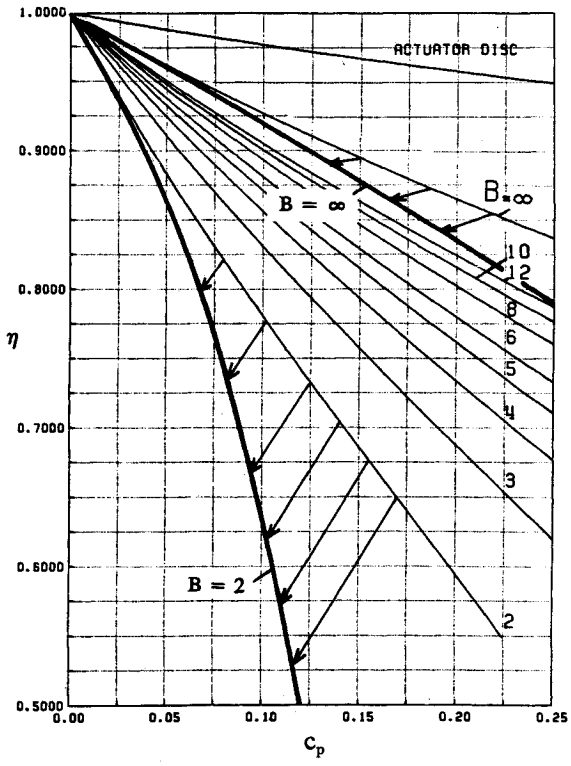

Fig. 3 Ideal η vs c_p at $\lambda = 1$; various numbers of blades B.

References

[1]Theodorsen, T., *Theory of Propellers*, McGraw-Hill, New York, 1948.

[2]Betz, A., "Schraubenpropeller mit geringsten Energieverlust," *Mitt. Nachr. d. Kgl. Ges. d. Wiss. zu Göttingen. Math. Phys. Klasse*, Heft 2, 1919; see also Prandtl, L., Appendix to Ref. 2.

[3]Schouten, G., "Static Pressure in the Slipstream of a Propeller," *Journal of Aircraft*, Vol. 19, No. 3, 1982, pp. 251, 252.

[4]Ribner, H. S., and Foster, S. P., "Ideal Efficiency of Propellers: Theodorsen Revisited," *Journal of Aircraft*, Vol. 27, No. 9, pp. 810–819.

[5]Kramer, K. N., "The Induced Efficiency of Optimum Propellers Having a Finite Number of Blades," Luftfahrtforschung, Vol. 15, 1938, pp. 326–333; see also NACA TM 884.

[6]Aris, R., *Vectors, Tensors, and the Basic Equations of Fluid Mechanics*, Prentice-Hall, Englewood Cliffs, NJ, 1962, pp. 84–85.

Permeable Airfoils in Incompressible Flow

Virgil M. Musat*
Institute of Applied Mathematics of the Romanian Academy, Bucharest, Romania

Nomenclature

C_L = lift coefficient
c = chord of airfoil
c_p = pressure coefficient
c_{pc} = pressure coefficient in cavity
M = freestream Mach number
p = porosity
Re = Reynolds number
s = length of permeable region
V = total velocity
x, z = Cartesian coordinates
α = incidence angle

Introduction

THE improvement of aircraft's handling in stall and the increasing of lift are two major aims in aircraft design. A possibility of attaining these seems to be with the use of airfoils with a permeable region, which work like self-adapting airfoils.

The idea of utilizing permeable regions for diminishing the pressure gradient through shock waves on airfoils in transonic flows was initiated by Savu and Trifu.[1] Great pressure gradients also appear at high incidences and, therefore, it seems reasonable to use permeable regions in incompressible flows.

Real flows over airfoils, especially at high incidences, represent an adaptation of the potential flow to the special conditions induced by viscosity. Attached flow regions are in the neighborhood of separated flow regions, like that of long bubbles. The basic idea in this note is to use, from the real flow, the effects of bubbles to improve the performances of the airfoils, especially at high incidences. In this manner, self-adaptive airfoils can be obtained, with lift close to that in potential flow.

The interaction between the external and internal flow in an unventilated cavity (see Fig. 1) through a permeable boundary, give rise to a "provoked bubble." The form and height of this bubble is the function of the external pressure and the permeability function p. In the potential model, the provoked bubble has three functions: 1) the diminution of leading edge peak, 2) the diminution of positive pressure gradient after peak, and 3) the increase of airfoil lift. In other words, the role of the provoked bubble is to smooth the pressure distribution. It is expected that all these functions could enhance the boundary-layer capability and therefore improve the behavior of the airfoil near stall.

Analysis

A zonal solution method (Fig. 1) was adopted. For the secondary flow in a cavity and bubble, and for the principal inviscid flow around the airfoil, a potential model was considered. For the viscous flow on the airfoil and the bubble boundary it was considered the boundary-layer model.

A secondary self-adapting flow borns, in the leading-edge (l.e.) region, because of the pressure gradient through the permeable region. This flow is subject to the Darcy law

$$V_n = p(c_p - c_{pc}) \tag{1}$$

which states that the normal velocity V_n, on a permeable surface is proportional to the pressure gradient between its

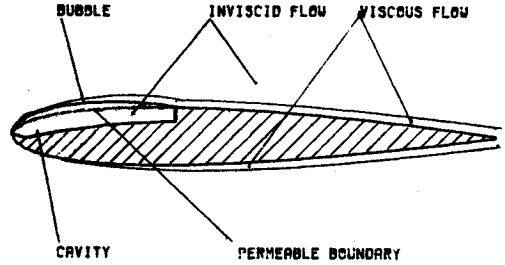

Fig. 1 Permeable airfoil.

Received Feb. 8, 1992; revision received May 13, 1992; accepted for publication May 22, 1992. Copyright © 1991 by the American Institute of Aeronautics and Astronautics, Inc. All rights reserved.

*Research Scientist, CFD Department.

two sides. For an unventilated cavity the mass rate over the entire permeable region is zero:

$$\int_s V_n \, ds = 0 \tag{2}$$

From the Bernoulli's law and Eqs. (1) and (2) the constant velocity in cavity V_c is given by the following equation:

$$V_c^2 = \left(\int_s V^2 p \, ds \Big/ \int_s p \, ds \right) \tag{3}$$

An iterative procedure for the calculation of the velocities V_n, V_c, and V is followed using Eqs. (1) and (3).

A surface singularity method,[2] which has a proven accuracy, efficiency, and generality, was adopted to solve the principal inviscid flow. The airfoil is approximated by a polygon with 2N sides (N number of panels on the upper surface) and the singularity distribution by piecewise continuous functions defined on panels. The source distribution is specified as constant on each panel and the vorticity is allowed to vary linearly. The source and vortex density on opposite panels on the upper and lower surface are taken as equal. For separated flows, in the trailing-edge region, a very simple model was used. From the separation point, the airfoil is approximated by a horizontal line. On this line are disposed sources so that the velocity on it remains equal with that at the separation point. By an iterative procedure in the hypothesis of small perturbations, the intensities of sources are obtained.

For solving the viscous flow an integral method was adopted which is simple, rapid, and has a proven accuracy. The boundary-layer development—laminar, transition to turbulent, and entirely turbulent—is calculated along both upper and lower surfaces of airfoil, from the stagnation point to the separation point or trailing edge. The laminar boundary layer is calculated by an extension of Thwaites method[3] for compressible flows. The turbulent boundary layer is calculated by Sasman-Cresci's method.[4]

A direct interactive method was adopted for matching the inviscid and viscous flows. The iterative coupling between inviscid and viscous flow is obtained by boundary condition modification with the transpiration velocity. This transpiration velocity is superposed on the normal local velocity corresponding to the permeable or separated region. The advantage in computer time of this procedure results from having to calculate the influence coefficients only once. At each successive interation, only matrix multiplication is required to determine the new singularity strengths. For attached flows, the iterative procedure is under-relaxed and the convergence is achieved when the average relative error of the velocity on the entire airfoil is less than a given value. For detached flows the viscous-inviscid matching is approximated very crudely. Thus, it is considered that the convergence is achieved when the separation points coincide at two successive iterations.

Results and Conclusions

The flow over a NACA 0012 airfoil with and without a permeable region at $M = 0.2$ and $Re = 6 \times 10^6$ was numerically studied with the INTVN code.[5]

The pressure distribution on an airfoil with a constant permeability ($p = 0.15$) region, from l.e. to 39% of chord, at $\alpha = 13$ deg incidence is shown in Fig. 2. The geometry of the airfoil and the provoked bubble are also drawn. The hollow which appears at the end of the permeable region is a result of a great suction. The lift variation with the incidence angle is presented in Fig. 3 for the solid and permeable airfoil in viscous flow and for the solid airfoil in potential flow. It can be observed that the theoretical results obtained with the INTVN code are in close agreement with experimental data

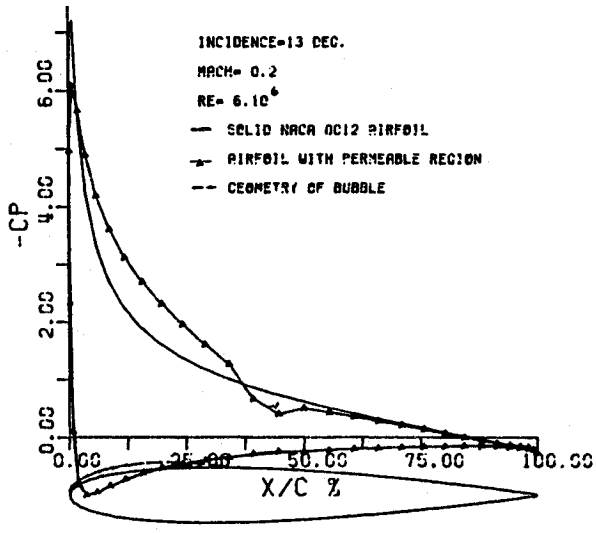

Fig. 2 Pressure distribution on airfoil with constant porosity region.

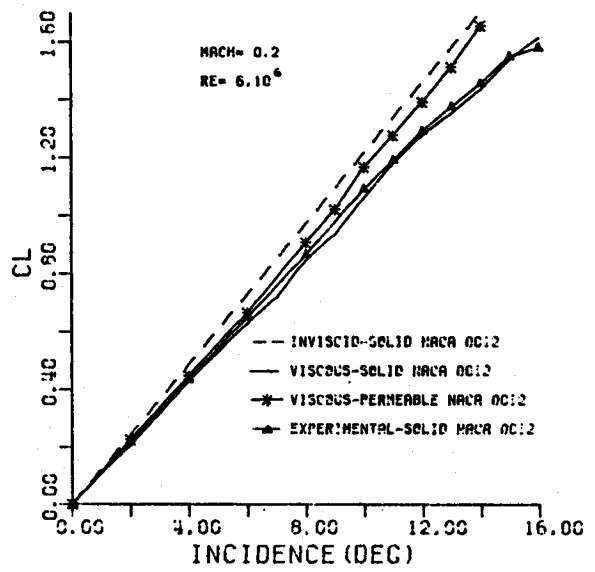

Fig. 3 Variation of lift as a function of α.

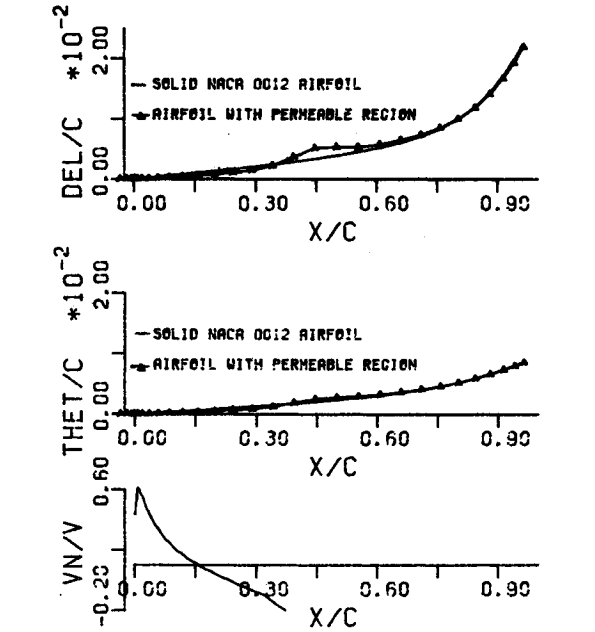

Fig. 4 Local quantities on upper surface of airfoil: a) displacement thickness, b) momentum thickness, c) normal velocity V_n.

from Abbott and Doenhoff[6] (solid airfoil). The provoked bubble increases the lift with about 10% and tends to bring the lift curve near that of potential flow. At incidences higher than 13 deg, when the flow separates, the very simple flow model does not work well. In Figs. 4a and 4b, the displacement and momentum thickness on the upper surface of the airfoil, at 13-deg incidence, are presented. On the entire permeable region, the displacement and momentum thickness are thinner for the permeable airfoil. Only at the end of this region, is there an increase which is the result of the pressure hollow. The V_n in the permeable region, is shown in Fig. 4c. A great suction can be observed at the end of the permeable region (negative normal velocity) which can be helpful for the behavior of the boundary layer. The diminution of the positive pressure gradient after the l.e. peak, determines a delay in transition on the upper surface of the airfoil.

These theoretical results, obtained using a simple flow model, are encouraging. They must be verified by a more complex flow model for detached regions and especially by comparison with experiments.

References

[1]Savu, G., and Trifu, O., "Porous Airfoils in Transonic Flow," *AIAA Journal*, Vol. 22, No. 7, 1984, pp. 989–991.

[2]Musat, V. M., "A Simple Integral Method of Potential Flow Analysis Around Airfoils" (in Romanian), *Studii si Cercetari de Mecanica Aplicata*, Vol. 51, No. 1, 1992, pp. 49–59.

[3]Rosenhead, L., "Laminary Boundary Layers," Clarendon Press, Oxford, England, UK, 1963, pp. 303–308.

[4]Sasman, P. K., and Cresci, R. J., "Compressible Turbulent Boundary Layer with Pressure Gradient and Heat Transfer," *AIAA Journal*, Vol. 4, No. 1, 1966, pp. 19–25.

[5]Musat, V. M., "A Direct Viscous-Inviscid Interaction Method for the Flow Calculation Around Airfoils," *Revue Roumaine des Sciences Techniques, Serie de Mecanique Applique*, Vol. 37, No. 3, 1992, pp. 17–29.

[6]Abbott, I. H., and Von Doenhoff, A. E. N., "Theory of Wing Sections," Dover, New York, 1958, pp. 462–463.

Dynamic Stability Derivatives Evaluation in a Low-Speed Wind Tunnel

G. Guglieri*
National Research Council, Torino, Italy
and
F. B. Quagliotti†
Turin Polytechnic Institute, Torino, Italy

Introduction

THE origin of the program developed at TPI/TU is that, with the improvement in fighter aircraft maneuverability, the analysis of flight at high angles of attack and in poststall conditions has become more relevant. As a consequence, the dynamic derivatives evaluation becomes even more important for the recent aircraft configurations. In particular, the measurement of dynamic stability derivatives has been refined in order to investigate the nonlinearities of the aerodynamic coefficient trends as a function of motion variables.

One of the most widely used methods to obtain dynamic stability parameters is the direct forced oscillation technique, where the model oscillates at constant amplitude and frequency in a single degree of freedom (DOF). Therefore, any aerodynamic reaction is supposed to be coherent with the primary motion. Hence, a direct causal relationship between the aerodynamic reactions and the primary motion itself is established, when small angular displacements are considered. This condition permits a rather simple determination of the derivatives, as discussed in Ref. 1.

In this note, a set of experimental results—obtained with the new TPI/TU rig—is presented. These data reproduce, with small discrepancies, the measurements on similar calibration models, performed by NRC/IAR, DLR, and FFA.

Experimental Facilities

The TPI/TU D3M low-speed wind tunnel is a closed-circuit tunnel with a contraction ratio of 5.44. The test section is circular with a 3-m diameter. The maximum speed is 98 m/s and the turbulence level is 0.3% at 50 m/s.

The propelling system is driven by a 1.1-MW dc motor and it consists of two fans with four blades that are mechanically linked to the motor by a gear box.

The model tested was the standard dynamics model (SDM). This is a calibration model introduced by NRC/IAR in 1978, specifically for dynamic tests. The weight of the model (machined in aluminum alloy) without the internal balance is 8 kg. The wing surface is trapezoidal with a 40-deg sweep angle and the main geometrical dimensions are length 0.943 m, wing span 0.609 m, wing surface 0.117 m^2, and mean aerodynamic chord 0.220 m. The center of gravity (c.g.) of the oscillating system (i.e., balance reference center) is at 35% of the mean aerodynamic chord.

A specific servomechanical unit (see Fig. 1) was designed in order to perform static tests on the model and to generate the harmonic motion of the SDM in the three separate rotational DOF. The final design of the unit was the result of previous experience and development.[2,3]

A vertical strut supports the model that is connected to a strain gauge balance by an internal leverage that links the

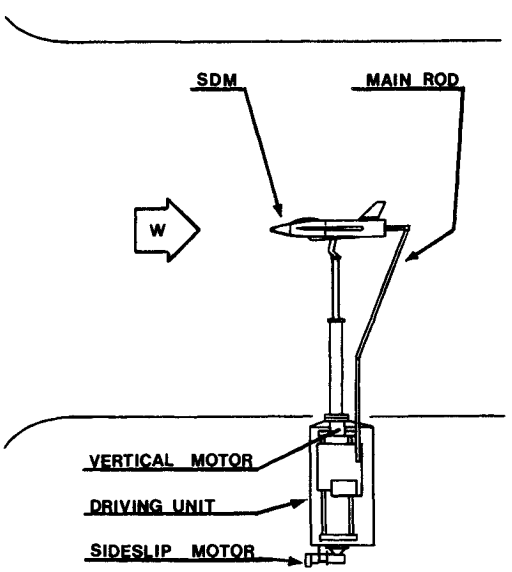

Fig. 1 TPI/TU mechanical apparatus.

Presented as Paper 91-3245 at the AIAA 9th Applied Aerodynamics Conference, Baltimore, MD, Sept. 23–26, 1991; received Feb. 19, 1992; revision received June 15, 1992; accepted for publication June 15, 1992. Copyright © 1991 by the American Institute of Aeronautics and Astronautics, Inc. All rights reserved.

*Scientist Researcher, Centro Studi Dinamica Fluidi. Member AIAA.

†Associate Professor, Aerospace Engineering Department. Member AIAA.